ISSN 1070-3632, Russian Journal of General Chemistry, 2014, Vol. 84, No. 4, pp. 775–781. © Pleiades Publishing, Ltd., 2014.

Effect of the Nature of Conductive Supported Nickel Electrocatalyst for Salicylic Acid Oxidation in Alkaline Medium[1]

M. Doulache and A. Benchettara

Laboratory of Electrochemistry-Corrosion, Metallurgy, and Inorganic Chemistry, Faculty of Chemistry, (USTHB) BP 32, El Alia, Algiers 16111 Algeria
e-mail: doulache@yahoo.fr

Received March 31, 2014

Abstract—The electrocatalytic activity of Ni films electrodeposited on glassy carbon (Ni/GC), titanium (Ni/Ti), and gold (Ni/Au) electrodes toward salicylic acid (SA) oxidation are investigated. The cyclic voltammetry studies show that the nature of substrate strongly influences the apparent electrocatalytic activities of the nickel over layer in basic medium. It is observed that the Ni/GC electrode has higher activity for SA oxidation compared to other electrodes. Effects of various parameters such as concentration of Ni^{2+}, deposition time for Ni film growth, and deposition potential on the electrooxidation of SA are investigated. It is demonstrated that the $Ni(OH)_2$/NiOOH plays the key role in the electrooxidation of SA. The response to SA on the Ni/GC electrode is examined using chronoamperometry.

DOI: 10.1134/S107036321404029X

INTRODUCTION

Salicylic acid (SA) is a biological substance widely used in cosmetics, lotions, and drugs owing to its antiseptic, antipyretic and anti-inflammatory properties [1–3]. Many analytical methods for the SA determination have been reported in the literature like the UV-Vis spectrophotometry [4, 5], spectrofluorimetry [6], combined gas chromatography-mass spectrometry [7], and high-performance liquid chromatography (HPLC) [8, 9]. However, such techniques require sample pretreatment, complicated operations and often show poor efficiency. So, there is a need to develop a simple and convenient method for SA titration by using an electrochemical technique (potentiometry, amperometry, and voltammetry), which have proved their effectiveness in the analytical chemistry. The electrochemical detection of SA at bare electrodes (Pt, Au, carbon paste and graphite) is not suitable for analytical applications due to the slow electron transfer and high over-potentials [10, 11]. In addition, they are prone to electrode fouling, low sensitivity, and poor reproducibility. More recently, the chemical and electrochemical modifications of electrodes with electron transfer mediators offered significant advantages for the design and development of electrochemical sensing devices. Therefore, there is a great interest in the area of modified electrodes to overcome these problems, and various materials have been elaborated for this purpose [12–15].

In this respect, the oxide and oxyhydroxide films of transition metals have been successfully used for technological applications including bioelectronics, catalysis, optics, biomedical, as well as chemical and biochemical sensors due to their electrocatalytic activity toward organic molecules and roughness of the sensing interface [16–19]. Among 3*d* metals, nickel-based electrodes, including nickel bulk metal [20], nickel hydroxide [21], nickel nanoparticles [22], nickel oxide [23], nickel alloys [24, 25] and nickel complexes [26–28] have been used for the oxidation of organic and biological molecules. Their oxidation involves the formation of high nickel valences, acting as chemical oxidizing agent and the β-$Ni(OH)_2$/β-NiOOH couple works as an effective electron mediator [23]. A catalytic reaction mechanism has been generally used to explain the results obtained in the electrooxidation of several organic molecules at oxy-hydroxide modified metal electrodes [21, 24]. According to this mechanism, $Ni(OH)_2$ is first oxidized to NiOOH, which then reacts with the organic molecule to regenerate the starting material. The proposed general mechanism can be represented as:

[1] The text was submitted by the authors in English.

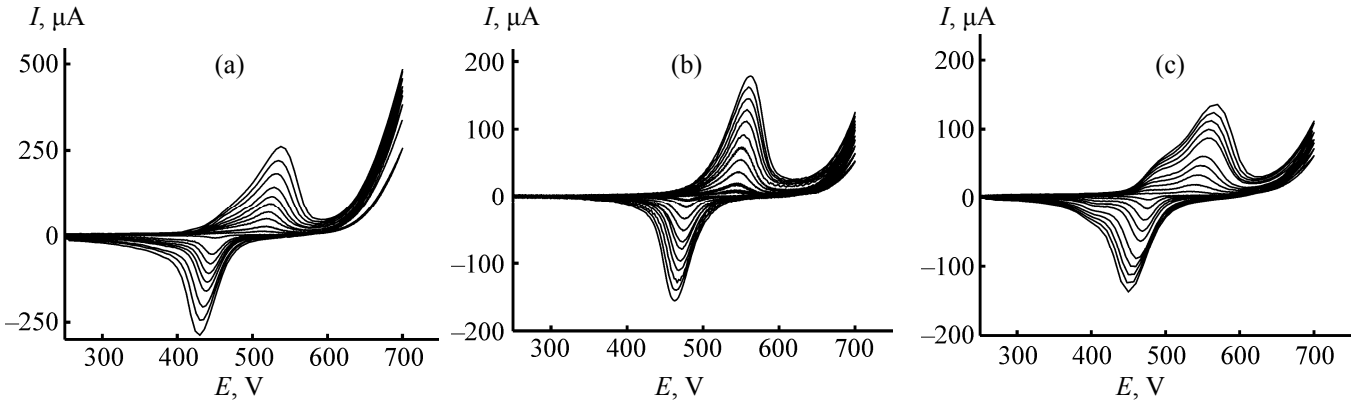

Fig. 1. Cyclic voltammetry response of (a) Ni/GCE, (b) Ni/Ti, and (c) Ni/Au in NaOH (0.1 M) solution at different scan rates: 10, 25, 50, 75, 100, 125, 150, 200, 250, and 300 mV s^{-1}.

$$Ni(OH)_2 + OH^- \leftrightarrow NiOOH + H_2O + e, \quad (1)$$

$$NiOOH + \text{organic molecule} \rightarrow Ni(OH)_2 + \text{products}. \quad (2)$$

Formation of a nickel hydroxide layer on a substance can be performed using several electrochemical methods such as: (a) applying a large number of potential sweeps to a nickel electrode in alkaline solution [29, 30], galvanostatic oxidation of nickel in alkaline media [31], deposition of $Ni(OH)_2$ layers on a negative electrode during the electrolysis of pH-controlled $Ni(NO)_3$ solution without either nickel metal deposition or hydrogen gas evolution [32], andplacing a droplet of Ni^{2+} solution on the surface of the electrode, evaporating the solvent, transferring to an alkaline medium, and potential sweeping in the region of nickel oxide formation [33]. In these manners, a very low soluble nickel oxide layer is attached to the surface.

This result prompted us to obtain thin electrodeposited films of Ni on different substrates, namely, glassy carbon (GC), Au and Ti and to investigate their electrocatalytic properties towards the SA oxidation in alkaline medium. The present paper reports the details of results of the investigation.

EXPERIMENTAL

All chemicals are analytical-grade reagents, and the solutions are prepared with doubly distilled water. $NiSO_4$, salicylic acid (99.5%), H_3BO_3 and NaOH are purchased from Fluka. The phosphate buffer solutions (0.1 M) are prepared form H_3PO_4, NaH_2PO_4, and Na_2HPO_4. The pH is adjusted to the desired value with HCl and NaOH solutions and monitored by a digital pH meter (Hanna pH 211).

Electrochemical measurements are performed in three-electrode cell with a PGZ301 potentiostat/galvanostat (Radiometer analytical). The temperature is regulated at 25 ± 0.5°C with a thermo stated bath. Modified Ni/GC, Ni/Au, Ni/Ti and bare GC are used as working electrodes, a platinum sheet as auxiliary electrode and Ag/AgCl (sat KCl) as reference electrode. Each test is repeated three times to confirm the reproducibility of the results. For steady-state amperometric experiments, the working potential is fixed at 0.55 V and the solution is stirred gently by magnetic agitation.

The substrates (GC, Au, and Ti) are polished with Al_2O_3 slurry (1.0 and 0.4 μm) and thoroughly washed with water until a mirror-like surface is obtained. Then, they are cleaned ultrasonically in 1 : 1 nitric acid/absolute ethanol (5 min), rinsed with distilled water and dried at room temperature. Afterward, the electrodes are cycled between 0 and +1 V in H_2SO_4 (0.1 M) with a scan rate of 50 mV s^{-1}. The Ni films are first deposited electrochemically on the surface of support electrodes by cathodic reduction in a mixed solution [$NiSO_4$ (0.014 M)/H_3BO_3 (0.05 M), pH 5.25] by applying a potential of –1 V at different times (10–300 s). After rinsing with water, the modified electrodes are immersed in NaOH (0.1 M) solution and scanned for 10 cycles within the potential range (0.25–0.75 V) at 50 mV s^{-1} until a stable cyclic voltammogram (CV) is reached.

RESULTS AND DISCUSSION

Figure 1 demonstrates cyclic voltammograms (CVs) of Ni/GCE (a), Ni/Ti (b) and Ni/Au (c) in NaOH (0.1 M) at different scan rates (10–300 mV s^{-1}).

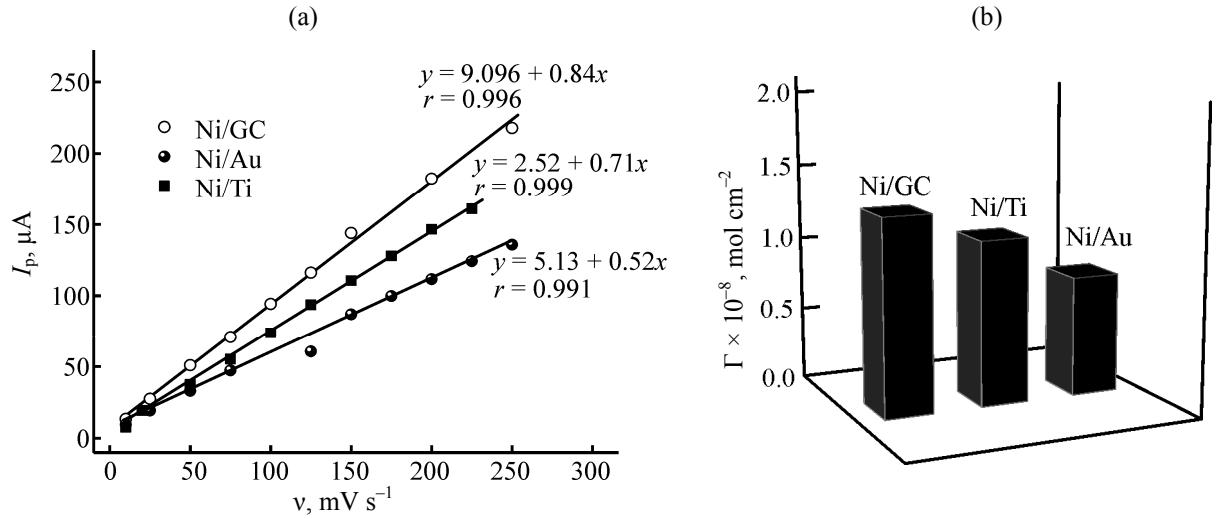

Fig. 2. (a) Plots of anodic peak currents vs. the scan rate of Ni/GCE, Ni/Au and Ni/Ti and (b) effects of the nature of substrate on surface coverage.

It can be seen that both anodic and cathodic peaks are observed on the three studied electrodes. The fact that there are redox-active substances present in the solution implies a deposition of the Ni onto the studied substrates. Therefore, the oxidation and reduction responses for the Ni film can be assigned to the Ni^{III}/Ni^{II} couple [20–22]. The proposed redox process may be represented by the following equation:

$$Ni(OH)_2 + OH^- \leftrightarrow NiO(OH) + H_2O + e. \quad (3)$$

In addition, it appeared that the anodic peak potential shifted towards the positive direction with an increase in scan rate, while the cathodic peak shifted towards a more negative potential. It is observed that the anodic and cathodic peak currents are dependent on scan rate. This behavior is depicted in Fig. 2a. A linear relationship of the plot between the anodic peak current (I_p) and the scan rates (10–250 mV s^{-1}) is established. This indicates an electrochemical activity of the surface redox couple [34]. The surface coverage (Γ) of Ni(III) species on different substrates is estimated from the Laviron's equation [34].

$$I_p = n^2F^2A\Gamma\nu(4RT)^{-1}, \quad (4)$$

where A is the electrode surface area, F the Faraday constant (95487 C mol^{-1}), n the number of exchanged electrons, T the absolute temperature, and R the universal gas constant. Based on values of Γ (Fig. 2b), the content of dispersed electro-active Ni(III) species on different substrates followed the order: Ni/GC > Ni/Ti > Ni/Au. These results show that the nickel particles dispersed on GCE substrate surface can provide more active sites for SA oxidation to increase the current responses. On the basis of the observation we presume that the Ni/GC electrode shows significantly greater electrocatalytic activity towards SA oxidation than Ni/Ti and Ni/Au.

The electrocatalytic activity of Ni film deposited on different substrates to the oxidation of SA is examined by cyclic voltammetry. Figure 3 shows the cyclic voltammograms at bare GC, Ni/Au, Ni/Ti, and Ni/GC in the absence (curves *a, c, e, g, i*) and presence (curves *b, d, f, h, j*) of SA (10 mM).

In the absence of SA, there is no electrochemical response at bare GC (curve *a*). But in the presence of SA, there is a broad, weak and irreversible oxidation peak of SA at 0.61 V (curve *b*), indicating a slow electrochemical reaction process. On the contrary, on Au, Ti, and GCE supported nickel (curves *c, e*, and *g*), a pair of peaks corresponding to the reversible Ni^{III}/Ni^{II} redox reaction is observed in the absence of SA. After addition of SA (curves *d, f,* and *h*), the anodic peak current increases significantly and the response current remains stable after the fourth cycle. This oxidation is accompanied by a decrease in the cathodic peak current, indicating a catalytic effect of the Ni^{III}/Ni^{II} redox couple toward SA oxidation. Furthermore, when the scan rate is 50 mV s^{-1}, the cathodic peak appears during the reverse scan, but it disappears completely at a low scan rate (i. e., 5 mV s^{-1}). This result demonstrates that at the low scan rate, the entire Ni(III) species in the surface layer gets reduced to Ni(II) species through interaction with SA/intermediate and

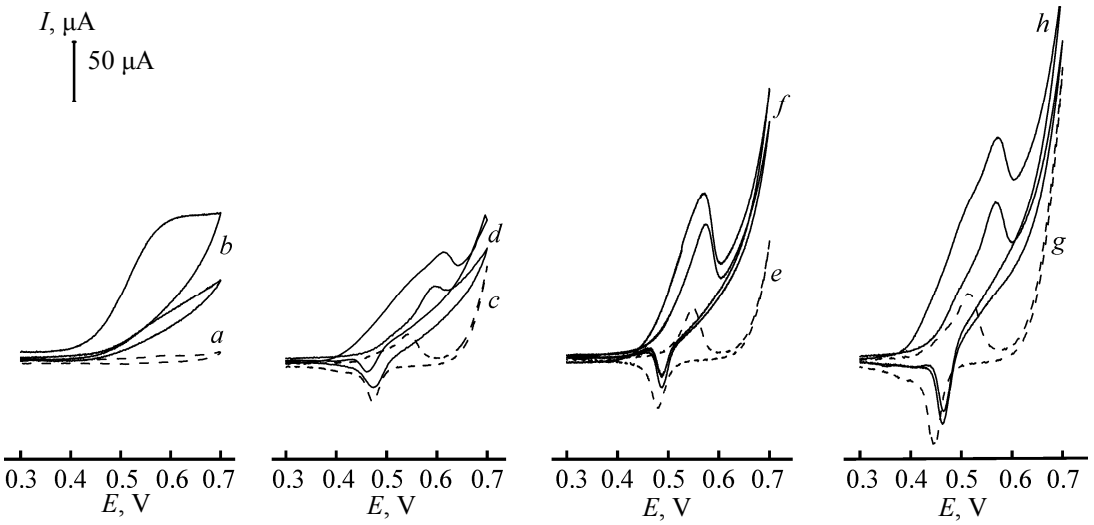

Fig. 3. Cyclic voltammograms of GCE (*a* and *b*), Ni/Au (*c* and *d*), Ni/Ti (*e* and *f*) and Ni/GCE in NaOH (0.1 M; pH 13) in the absence (*a, c, e, g*) and presence (*b, d, f, h*) of SA (10 mM). Scan rate: 50 mV s^{-1}.

there is almost nil Ni(III) species left for electrochemical reduction to Ni(II) under cathodic condition. The stabilization of the peak current at to the fourth scan is likely due to a stationary state of the diffusion controlled anodic process [14]. Based on values of the anodic peak current, the electrode followed the electrocatalytic order: Ni/GCE (137.68 μA) > Ni/Ti (116.98 μA)> Ni/Au (65.81 μA). Comparatively, Ni/GCE is more suitable for the detection of SA.

To further investigate the influence of the nature of support on the electrocatalytic activity of Ni catalyst, the exchange current density (i_0) of SA oxidation at three electrodes is investigated in NaOH (0.1 M) + SA (10 mM) aqueous solution. The polarization studies have been carried out and the typical Tafel curves are shown in Fig. 4. The values of i_0 at Ni/GCE, Ni/Ti and Ni/Au electrodes are calculated according to the Tafel curves and equal to 425.71, 265.57, and 186.04 μA cm^{-2},

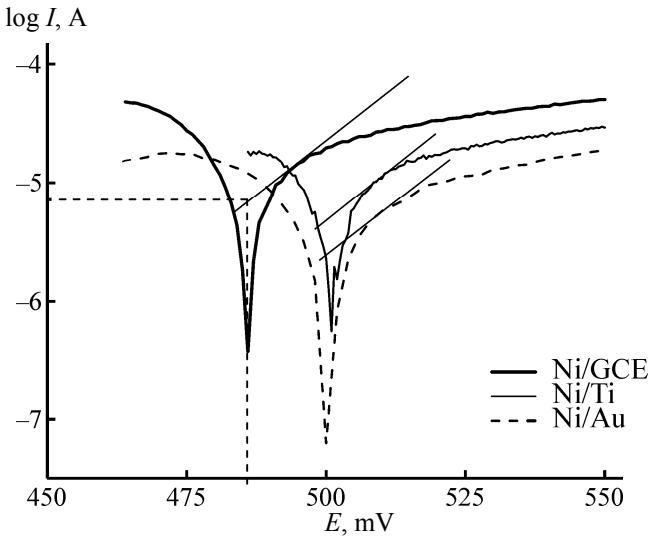

Fig. 4. Tafel plots of the Ni/GCE, Ni/Ti and Ni/Au in NaOH (0.1 M) + SA (10 mM) aqueous solutions. Scan rate: 5 mV s^{-1}.

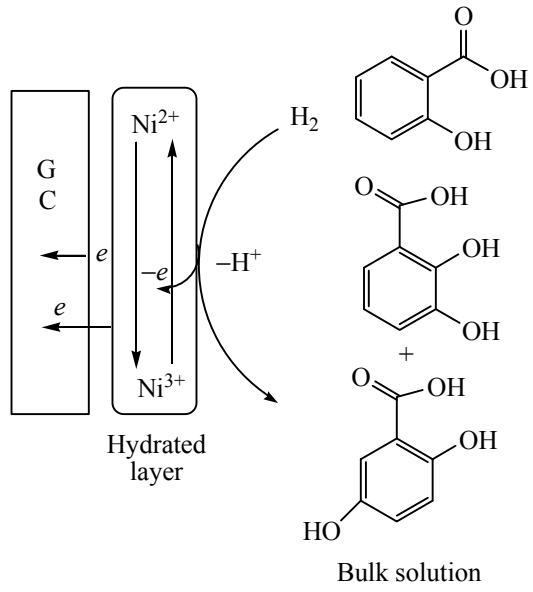

Fig. 5. The electrocatalytic oxidation mechanism of SA at Ni/GCE.

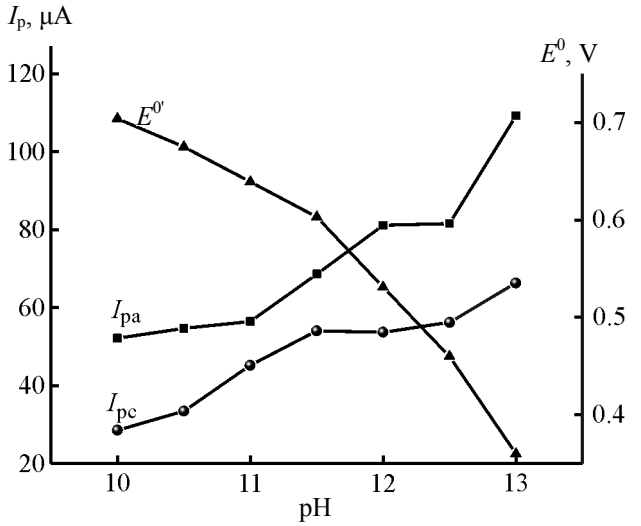

Fig. 6. Influence of pH on the peak current Ip and peak formal potential $E^{0'}$ of Ni/GCE; scan rate 50 mV s^{-1}.

respectively. Based on the i_0 values, the Ni/GCE is found to be the greatest active electrode for the SA electrooxidation.

Based on our results and the work of Ai et al. [35], the following mechanism can be proposed for the mediated oxidation of SA on the modified surface, which is outlined in Fig. 5. The redox transition of nickel species is:

$$\text{Ni(II)} \leftrightarrow \text{Ni(III)} + e. \quad (5)$$

In addition, SA is oxidized on modified surface via the following reaction:

$$\text{Ni(III)} + \text{SA} \rightarrow \text{Intermediate} + \text{Ni(II)}, \quad (6)$$

where the intermediate is further oxidized to the product, 2,3-dihydroxylated benzoic acid or 2,5-dihydroxylated benzoic acid, through the final electron transfer process:

$$\text{Ni(III)} + \text{Intermediate} \rightarrow \text{Product} + \text{Ni(II)}. \quad (7)$$

To investigate the contribution of OH^- in the electrochemical process of Ni/GC electrode, the effect of pH on the voltammetric behavior is studied in the pH range (10–13). With increasing pH, both the anodic and cathodic current peaks increase and the formal potential ($E^{0'}$) of the redox couple shifts to less positive potentials (Fig. 6), suggesting that OH^- participates in the redox process on the modified electrode.

To get the best response for the SA electrooxidation on Ni/GC in NaOH solution, the effects of Ni^{2+} concentration, deposition time, and deposition potential

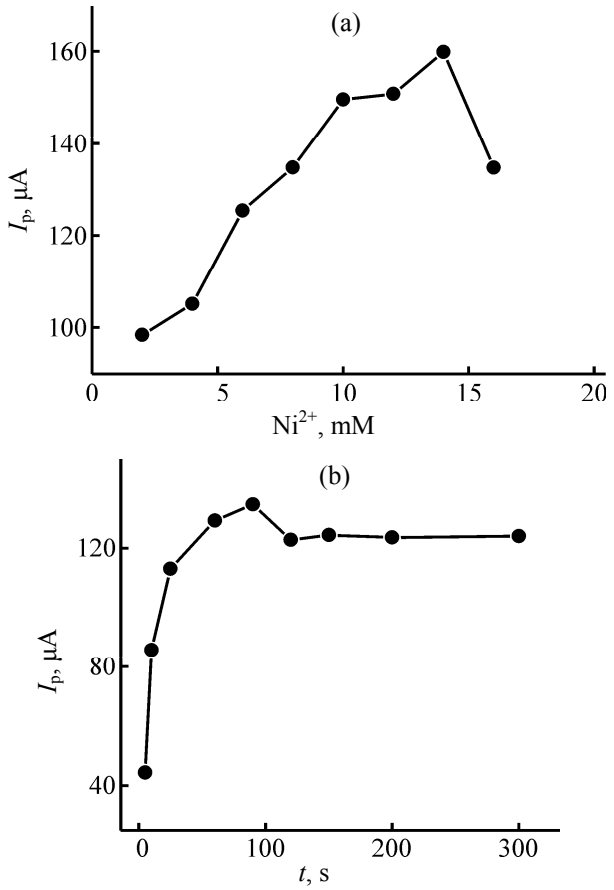

Fig. 7. Effect of $NiSO_4$ concentration (a) and the deposition time (b) for nickel film formation on the electrocatalytic activity of Ni/GCE. The concentration of SA: 10 mM.

are investigated by CV. Figure 7a shows the influence of Ni^{2+} concentration for the nickel film deposition on the activity of Ni/GCE. The electrocatalytic current is high in the range (10–16 mM) with an optimal Ni^{2+} concentration of 14 mM, a result is due to combined interaction of active sites with the film resistance. Figure 7b shows the influence of deposition time for Ni film growth on the electrocatalytic activity of Ni/GCE which determines the film thickness. The nickel film does not cover completely the GCE surface for short times, leading to an insufficient number of active sites. For longer time, the morphology of electrodeposited nickel changes from particles islands to uniform film, which could decrease the active sites. An optimal deposition time of 90 s is found. The effect of deposition potential on the film response is investigated in the range (from –1.3 to –0.7 V). An optimal enrichment potential of –1.0 V is obtained (figure not shown).

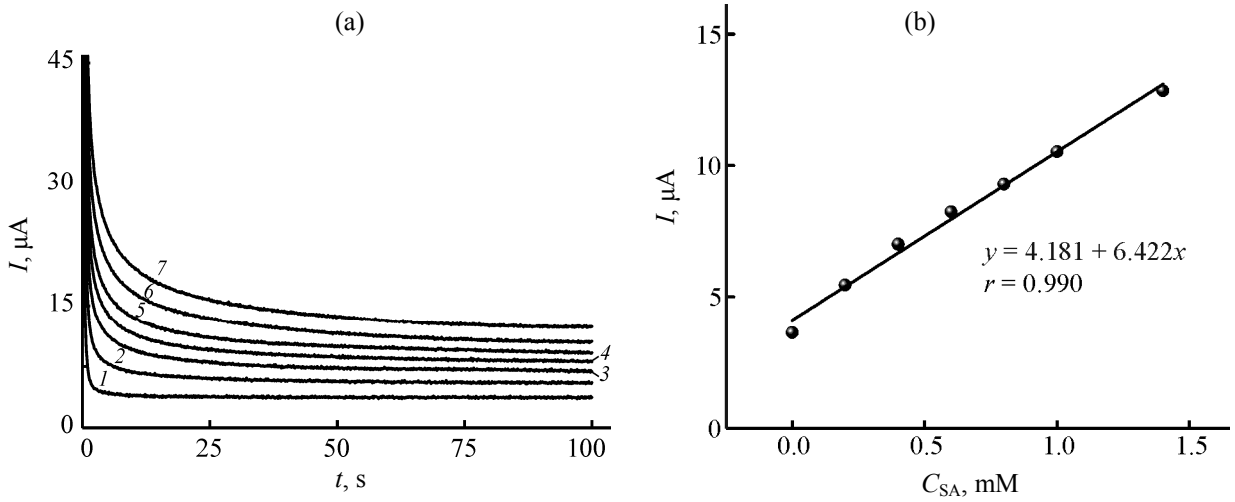

Fig. 8. Chronoamperograms obtained for Ni/GCE: (a) in the absence (*1*) and in the presence of (*2*) 0.2, (*3*) 0.4, (*4*) 0.6, (*5*) 0.8, (*6*) 1.0, and (*7*) 1.4 mM SA in NaOH (0.1 M) using a potential step of 550 mV; and (b) the variations of amperometric currents measured against SA concentration.

Chronoamperometry at Ni/GCE is used to study the SA oxidation. For this order, 550 mV potential step is applied to the Ni/GCE immersed in NaOH (0.1 M) containing various concentrations of analyte (0–1.4 mM). The corresponding chronoamperograms are presented in Fig. 8a. Under these conditions, the observed currents are controlled by rate of SA diffusion towards electrode surface [36].

The results shown in Fig. 8a indicate that, in the presence of SA, the currents increased as the SA concentration increasing. This result supports our conclusion about the catalytic role of Ni/GCE for SA oxidation. The linear dependence of amperometric responses to the SA concentrations allows us to suggest that the Ni/GCE can be used as an amperometric sensor for SA determination (Fig. 8b).

CONCLUSIONS

This study has demonstrated that the nature of support strongly influences the apparent electrocatalytic activity of the overlayer of dispersed Ni. Among the electrodes investigated, the Ni/GC electrode is found to have the greatest apparent electrocatalytic activity towards SA. It was demonstrated that the nickel particles dispersed on GCE substrate surface provide more active sites for SA oxidation to increase the current responses.

REFERENCES

1. Mikami, E., Goto, T., Ohno, T., Matsumoto, H., and Nishida, M., *J. Pharma. Biomed. Anal*., 2002, vol. 28, no. 7, pp. 261–267.
2. Abdolmohammad-Zadeh, H., Kohansal, S., and Sadeghi, G.H., *Talanta*, 2011, vol. 84, no. 6, pp. 368–373.
3. Saha, U., and Baksi, K., *Analyst*, 1985, vol.110, no. 3, pp. 739–741.
4. Ruiz-Medina, A., Fernàndez-de Córdova, M.L., Ortega-Barrales, P., and Molina-Díaz, A., *Int. J. Pharm*., 2001, vol. 216, no. 10, pp. 95–104.
5. Kokot, Z., and Burda, K., *J. Pharm. Biomed. Anal*., 1998, vol. 18, no. 5, pp. 871–875.
6. Marcelo, M.S., Marcello, G.T., and Ronei, J.P., *Talanta*, 2006, vol. 68, p. 1707.
7. Kakkar, T., and Mayersohn, M., *J. Chromatogr., B*, 1998, vol.718, no. 7, pp. 69–75.
8. Kees, F., Jehnich, D., and Grobecker, H., *J. Chromatogr., B*, 1996, vol. 677, no. 6, pp. 172–177.
9. Jena, J.F., Tsaia, Y.Y., and Yang, T.C., *J. Chromatogr., A*, 2001, vol. 912, no. 5, pp. 39–43.
10. Petrek, J., Havel, L., Petrlova, J., Adam, V., Potesil, D., Babula, P., and Kizek, R., *Russ. J. Plant. Physiol*., 2007, vol. 54, no. 7, pp. 553–559.
11. Torriero, A.A.J., Luco, J.M., Sereno, L., and Raba, J., *Talanta*, 2004, vol. 62, no. 5, pp. 247–251.
12. Wang, Z., Wei, F., Liu, S.Y., Xu, Q., Huang, J.Y., Dong, X.Y., Yu, J.H., Yang, Q., Zhao, Y.D., and Chen, H., *Talanta*, 2010, vol. 80, no. 5, pp. 1277–1281.
13. Wang, Z., Ai, F., Xu, Q., Yang, Q., Yu, J.H., Huang, W.H., and Zhao, Y.D., *Colloids Surf., B*, 2010, vol. 76, no. 6, pp. 370–374.
14. Gualandi, I., Scavetta, E., Zappoli, S., and Tonelli, D., *Biosens. Bioelectron*., 2011, vol. 26, no. 7, pp. 3200–3206.

15. Zhang, W.D., Xu, B., Hong, Y.X., Yu, Y.X., Ye, J.S., and Zhang, J.Q., *J. Solid State Electrochem.*, 2010, vol. 14, no. 6, pp. 1713–1718.
16. Holade, Y., Morais, C., Clacens, S.A., Servat, K., Napporn, T. W., and Kokoh, K.B., *Electrocatal.*, 2013, vol. 4, no. 8, pp. 167–174.
17. Shakkthivel, P. and Chen, S.M., *Biosens. Bioelectron*., 2007, vol. 22, no. 8, pp. 1680–1687.
18. Verlato, E., Cattarin, S., Comisso, N., Gambirasi, A., Musiani, M., and Gómez, L.V., *Electrocatal*., 2012, vol. 3, no. 5, pp. 48–52.
19. Shaidarova, L.G., Gedmina, A.V., Chelnokova, I.A., and Budnikov, G.K., *Russ. J. Appl. Chem*., 2007, vol. 80, no. 7, pp. 1346–1352.
20. Zhao, C., Li, M., and Jiao, K., *J. Anal. Chem*., 2006, vol. 61, no. 5, pp. 1204–1208.
21. Majdi, S., Jabbari, A., and Heli, H., *J. Solid State Electrochem*., 2007, vol. 11, no. 7, pp. 601–607.
22. Safavi, A., Maleki, N., and Farjami, E., *Biosens. Bioelectron*., 2009, vol. 24, no. 6, pp. 1655–1660.
23. Roushani, M., Shamsipur, M., and Pourmortazavi, S.M., *J. Appl. Electrochem*., 2012, vol. 42, no. 7, pp. 1005–1011.
24. Jafarian, M., forouzandeh, F., Danaee, I., and Gobal, F., *J. Solid State Electrochem*., 2009, vol. 13, no. 9, pp. 1171–1179.
25. Danaee, I., Jafarian, M., Mirzapoor, A., Gobal, F., and Mahjani, M.G., *Electrochim. Acta*, 2010, vol. 55, no. 8, pp. 2093–2100.
26. Elahi, M.Y., Heli, H., Bathaie, S.Z., and Mousavi, M.F., *J. Solid State Electrochem*., 2007, vol. 11, no. 10, pp. 273–282.
27. Gholivanda, M.B., Pashabadi, A., Azadbakht, A., and Menati, S., *Electrochim. Acta*, 2011, vol. 56, no. 9, pp. 4022–4030.
28. Zheng, L., and Song, J.F., *Anal. Biochem*., 2009, vol. 391, no. 8, pp. 56–63.
29. Jafarian, M., Mahjani, M.G., Heli, H., Gobal, F., and Heydarpoor, M., *Electrochem. Commun*., 2003, vol. 5, no. 7, pp. 184–190.
30. Kowal, A., Port, S.N., and Nichols, R.J., *Catal. Today*, 1997, vol. 38, no. 6, pp. 483–488.
31. MacDougall, B., Mitchell, D.F., and Graham, M.J., *J. Electrochem. Soc*., 1980, vol. 127, no. 5, pp. 1248–1252.
32. Wohlfahrt-Mehrens, M., Oesten, R., Wilde, P., and Huggins, R.A., *Solid State Ionics*, 1996, vol. 86, no. 5, pp. 841–849.
33. El-Shafei, A.A., J. *Electroanal. Chem*., 1999, vol. 471, no. 7, pp. 489–195.
34. Bard, A.J., and Faulkner, L.R., *Electrochemical Methods: Fundamentals and Applications*, John Wiley Press, 2001, 2 ed., p. 196.
35. Ai, S.Y., Wang, Q.J., Li H, and Jin, L.T., *J. Electroanal. Chem*., 2005, vol. 578, no. 7, pp. 223–229.
36. Hao-Yu, E., Scott, K., and Reeve, R.W., *J. Electroanal. Chem*., 2003, vol. 547, no. 9, pp. 17–25.